Restoring Degraded Face Images: A Case Study in Matching Faxed, Printed, and Scanned Photos

Thirimachos Bourlai, *Member, IEEE*, Arun Ross, *Senior Member, IEEE*, and Anil K. Jain, *Fellow, IEEE*

***Abstract*—We study the problem of restoring severely degraded face images such as images scanned from passport photos or images subjected to fax compression, downscaling, and printing. The purpose of this paper is to illustrate the complexity of face recognition in such realistic scenarios and to provide a viable solution to it. The contributions of this work are two-fold. First, a database of face images is assembled and used to illustrate the challenges associated with matching severely degraded face images. Second, a preprocessing scheme with low computational complexity is developed in order to eliminate the noise present in degraded images and restore their quality. An extensive experimental study is performed to establish that the proposed restoration scheme improves the quality of the ensuing face images while simultaneously improving the performance of face matching.**

***Index Terms*—Face recognition, faxed face images, image quality measures, image restoration, scanned face images.**

I. Introduction

A. Motivation

THE past decade has seen significant progress in the field of automated face recognition as is borne out by results of the 2006 Face Recognition Vendor Test (FRVT) organized by NIST [2]. For example, at a false accept rate (FAR) of 0.1%, the false reject rate (FRR) of the best performing face recognition system has decreased from 79% in 1993 to 1% in 2006. However, the problem of matching facial images that are severely degraded remains to be a challenge. Typical sources of image degradation include harsh ambient illumination conditions [3], low quality imaging devices, image compression, down sampling, out-of-focus acquisition, device or transmission noise, and motion blur [Fig. 1(a)–(f)]. Other types of degradation that have received very little attention in the face recognition literature include halftoning [Fig. 1(e)], dithering [Fig. 1(f)], and the presence of security watermarks on documents [Fig. 1(g)–(j)]. These types of degradation are observed in face images that are digitally acquired from printed or faxed documents. Thus, successful face recognition in the presence of such low quality probe images is an open research issue.

This work concerns itself with an automated face recognition scenario that involves comparing degraded facial photographs of subjects against their high-resolution counterparts (Fig. 2). The degradation considered in this work is a consequence of scanning, printing, or faxing face photos. The three types of degradation considered here are: 1) fax image compression,[1] 2) fax compression, followed by printing, and scanning, and 3) fax compression, followed by actual fax transmission, and scanning. These scenarios are encountered in situations where there is a need, for example, to identify legacy face photos acquired by a government agency that has been faxed to another agency. Other examples include matching scanned face images present in driver's licenses, refugee documents, and visas for the purpose of establishing or verifying a subject's identity.

The factors impacting the quality of degraded face photos can be 1) *person-related*, e.g., variations in hairstyle, expression, and pose of the individual; 2) *document-related*, e.g., lamination and security watermarks that are often embedded on passport photos, variations in image quality, tonality across the face, and color cast of the photographs; 3) *device-related*, e.g., the foibles of the scanner used to capture face images from documents, camera resolution, image file format, fax compression type, lighting artifacts, document photo size, and operator variability.

B. Goals and Contributions

The goals of this work include 1) the design of an experiment to quantitatively illustrate the difficulty of matching degraded face photos against high-resolution images, and 2) the development of a preprocessing methodology that can "restore" the degraded photographs prior to comparing them against the gallery face images. In this regard, we first propose an iterative image restoration scheme. The objective functions employed to guide the restoration process are two image distortion metrics, viz., peak signal-to-noise ratio (PSNR) and the Universal Image Quality Index (UIQ) proposed by Wang and Bovik [5]. The target is to generate restored images that are of higher quality and that can achieve better recognition performance than their

Manuscript received March 08, 2010; revised January 10, 2011; accepted January 11, 2011. Date of publication February 04, 2011; date of current version May 18, 2011. This work was supported by the Center for Identification Technology Research (CITeR) at World Class University (WCU). The work of A. K. Jain was supported in part by the WCU program through the National Research Foundation of Korea funded by the Ministry of Education, Science and Technology (R31-10008). A preliminary version of this work was presented at the First IEEE International Conference on Biometrics, Identity and Security (BIDS), September, 2009. The associate editor coordinating the review of this manuscript and approving it for publication was Dr. Fabio Scotti.

T. Bourlai and A. Ross are with the Lane Department of Computer Science and Electrical Engineering, West Virginia University, Morgantown, WV 26506 USA (e-mail: Thirimachos.Bourlai@mail.wvu.edu; Arun.Ross@mail.wvu.edu).

A. K. Jain is with the Computer Science and Engineering Department, Michigan State University, East Lansing, MI 48824 USA, and also with the Department of Brain and Cognitive Engineering, Korea University, Seoul 136-713, Korea (e-mail: jain@cse.msu.edu).

Color versions of one or more of the figures in this paper are available online at http://ieeexplore.ieee.org.

Digital Object Identifier 10.1109/TIFS.2011.2109951

[1]In this work, *Fax image compression* is defined as the process where data (e.g., face images on a document) are transferred via a fax machine using the T.6 data compression, which is performed by the fax software.

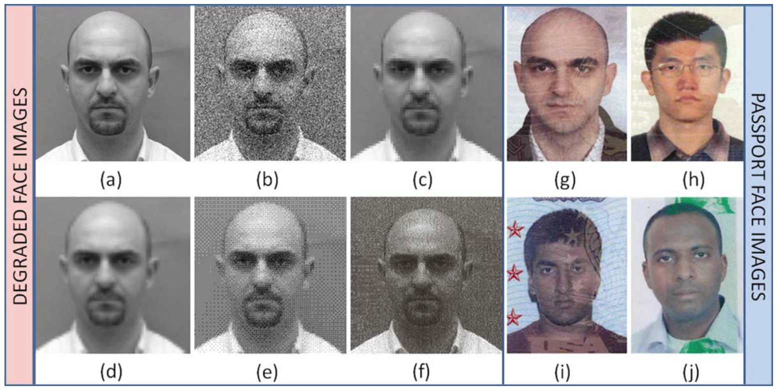

Fig. 1. Degraded face images: Low-resolution probe face images due to various degradation factors. (a) Original. (b) Additive Gaussian noise. (c) JPEG compressed (medium quality). (d) Resized to 10% and up-scaled to the original spatial resolution. (e) Half-toning. (f) *Floyd–Steinberg* dithering [4]. Mug-shots of face images taken from passports issued by different countries: (g) Greece (issued in 2006). (h) China (issued in 2008). (i) U.S. (issued in 2008). (j) Egypt (issued in 2005) [1].

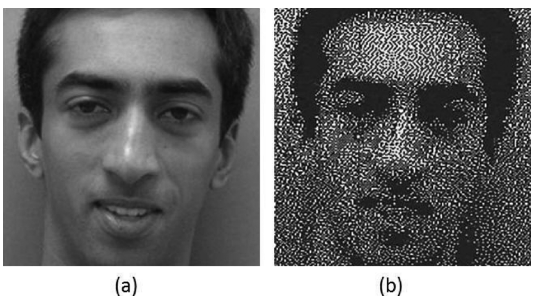

Fig. 2. Matching a high-resolution face image (a) against its degraded counterpart. The image in (b) is obtained by transmitting the document containing image (a) via a fax machine, and digitally scanning the resulting image.

original degraded counterparts. In order to facilitate this, a classification algorithm based on texture analysis and image quality is first used to determine the nature of the degradation present in the image. This information is then used to invoke the appropriate set of parameters for the restoration routine. This ensures that the computational complexity of both the classification and denoising algorithms is low, making the proposed technique suitable in real-time operations.

Second, we demonstrate that face recognition system performance improves when using the restored face image instead of the original degraded one. For this purpose, we perform *identification* tests on a variety of experimental scenarios, including 1) high-quality versus high-quality image comparison, and 2) high-quality versus degraded image comparison. In the high-quality versus high-quality tests, we seek to establish the baseline performance of each of the face recognition methods employed. In the high-quality versus degraded tests, we investigate the efficacy of matching the degraded face photographs (probe) against their high-resolution counterparts (gallery). Our approach avoids optimizing facial image representation purely for matching. Instead, the goal is to improve the quality of face images while at the same time boosting the matching performance. This can potentially assist human operators in verifying the validity of a match.

The key characteristics of the proposed face image restoration methodology are the following: 1) it can be applied on images impacted by various degradation factors (e.g., halftoning, dithering, watermarks, Gaussian noise, etc.); 2) individual images can have different levels of noise originating from a variety of sources; 3) the classification algorithm can automatically recognize the three main types of degradation studied in this paper; 4) it employs a combination of linear and nonlinear denoising methods (filtering and wavelets) whose parameters can be automatically adjusted to remove different levels of noise, and 5) the restoration process is computationally feasible (3 s per image in a Matlab environment) since parameter optimization is performed offline.

The proposed methodology is applicable to a wide range of face images—from high-quality raw images to severely degraded face images. To facilitate this study, initially a database containing passport photos and face images of 28 live subjects referred to as the WVU Passport Face Database was assembled. This dataset was extended to 408 subjects by using a subset of the FRGC2 [6] database. The purpose was to evaluate the restoration efficiency of our methodology in terms of identification performance on a larger dataset. Experiments were conducted using standard face recognition algorithms, viz., Local Binary Patterns [7], those implemented in the CSU Face Recognition Evaluation Project [8], and a commercial algorithm.

Section II briefly reviews related work in the literature. Section III presents the proposed restoration algorithm. Section V describes the technique used to evaluate the proposed algorithm. Section VI discusses the experiments conducted and Section VII provides concluding remarks.

II. Background

The problem addressed in this paper is closely related to two general topics in the field of image processing: 1) image restoration and 2) super-resolution. The problem of restoring degraded images has been extensively studied [9]–[15]. However, most of the proposed techniques make implicit assumptions about the type of degradation present in the input image and do not necessarily deal with images whose degree of degradation is as severe as the images considered in this work. Furthermore, they do not address the specific problem of restoring *face* images where the goal is to simultaneously improve image quality and recognizability of the face. In the context of super-resolution, the authors in [16] and [17] addressed the problem of matching a high-spatial resolution gallery face image against a low-resolution probe. With the use of super-resolution methods [18], high-resolution images can be produced from either a single low-resolution image [19] or from a sequence of images [20]. While such techniques can compensate for disparity in image detail across image pairs, they cannot explicitly restore noisy or degraded content in an image. Also, when using a single low-resolution image to perform super-resolution, certain assumptions have to be made about the image structure and content.

The problem of matching passport photos was studied in [21] where the authors designed a Bayesian classifier for estimating the age difference between pairs of face images. Their focus was on addressing the age disparity between face images prior to matching them. However, their work did not address the specific problem of matching face images *scanned from documents* such as passports. Staroviodov *et al.* [22], [23] presented an automated system for matching face images scanned from documents against those directly obtained using a camera. The authors constrained their study to an earlier generation of passports (1990s) from a single country. Further, in the images considered in their work, the facial portion of the photograph was reasonably clear and not "contaminated" by any security marks. Therefore, the system's ability to automatically identify the face photograph was not severely compromised. To the best of our knowledge, the only work reported in the literature that addresses the problem of passport facial matching using *international* passports is [1].

III. Face Image Restoration

Digital images acquired using cameras can be degraded due to many factors. Image denoising [24] is, therefore, a very important processing step to restore the structural and textural content of the image. While simple image filtering can remove specific frequency components of an image, it is not sufficient for restoring useful image content. For effective removal of noise and subsequent image restoration, a combination of linear denoising (using filtering), and nonlinear denoising (using thresholding) may be necessary in order to account for both noise removal as well as restoration of image features.

The quality of the denoiser used can be measured using the average mean square error $\mathrm{MSE}(\hat{h}, h_0) = E[(h_0 - \hat{h})^2]$, which is the error of the restored image $\hat{h}$ with respect to the true image h_0. Since the true image h_0 is unknown, the MSE corresponds to a theoretical measure of performance. In practice, this performance is estimated from denoising a single realization h using different metrics such as the PSNR and/or UIQ:

- **Signal-to-Noise Ratio** (SNR): It is a measure of the magnitude of the signal compared to the strength of the noise. It is defined (in units of decibels) as:

$$\mathrm{SNR}(\hat{h}, h_0) = -20 \cdot \log_{10} \cdot \frac{\|h_0\|}{\left\|\hat{h} - h_0\right\|}. \tag{1}$$

Fig. 3. Denoising using a Wiener filter of increasing width γ.

This measure of performance requires knowledge of the true signal h_0 that might not be available in a real scenario. Thus, it should only be considered as an experimentation tool. Furthermore, this metric neglects global and composite errors, and in a practical scenario, its use is questionable. As a result, one should observe the image visually to judge the quality of the denoising method employed.

- **Peak Signal-to-Noise Ratio** (PSNR): This measure is defined as the ratio between the maximum possible power of a signal and the power of corrupting noise that affects the fidelity of its representation. It is defined (in units of decibels) via the MSE as follows:

$$\mathrm{PSNR}(\hat{h}, h_0) = 10 \cdot \log_{10} \cdot \frac{\mathrm{MAX}_i{}^2}{\mathrm{MSE}(\hat{h}, h_0)} \tag{2}$$

where $\mathrm{MAX}_i{}^2$ is the maximum fluctuation in the input image data type. For example, if the image has a double-precision floating-point data type, then MAX_i is 1, whereas in the case of an 8-bit unsigned integer data type, MAX_i is 255. A higher PSNR would normally indicate that the reconstruction is of higher quality. However, the authors in [5] illustrate some limitations of MSE/PSNR, and thus one must be very cautious in interpreting its outcome [25].

- **Universal Image Quality Index** (UIQ): The measure proposed in [5] was designed to model any image distortion via a combination of three main factors, viz., loss of correlation [(3): term 1], luminance distortion [(3): term 2], and contrast distortion [(3): term 3]. In our study, UIQ can be defined as follows: given a true image x and a restored image y, let $\bar{x}, \bar{y}$ be the means, and σ_x^2, σ_y^2 be the variances of x and y, respectively. Also, let σ_{xy} be the covariance of x and y. Then, UIQ can be denoted as follows:

$$\mathrm{UIQ} = \frac{\sigma_{xy}}{\sigma_x \sigma_y} \cdot \frac{2\bar{x}\bar{y}}{\bar{x}^2 + \bar{y}^2} \cdot \frac{2\sigma_x \sigma_y}{\sigma_x^2 \sigma_y^2}. \tag{3}$$

A. Linear and Nonlinear Denoising

1) Image Filtering-Based Linear Denoising: Linear methods can be used for image denoising so that the noise that perturbs an image is suppressed as much as possible. The filtering strength can be controlled by the filter width γ: higher values of γ increase the blurring effect (see Fig. 3). When 2-D FIR filters are designed and used with the windowing method technique, γ represents the window size of the digital filter in terms of pixels. In this paper, several smooth window functions were tested, viz., Hamming, Hanning, Bartlett, Blackman, boxcar, Kaiser, and Chebwin, with variable window sizes. Linear methods can cause image blurring. Therefore, these filters are efficient in denoising smooth images but not images with several discontinuities.

2) Thresholding-Based Nonlinear Denoising: When wavelets are used to deal with the problem of image denoising [24], the necessary steps involved are the following: 1) Apply discrete wavelet transform (DWT) to the noisy image by using a wavelet function (e.g., Daubuchies, Symlet, etc.). 2) Apply a thresholding estimator to the resulting coefficients thereby suppressing those coefficients smaller than a certain amplitude. 3) Reconstruct the denoised image from the estimated wavelet coefficients by applying the inverse discrete wavelet transform (IDWT).

The idea of using a thresholding estimator for denoising was systematically explored for the first time in [26]. An important consideration here is the choice of the thresholding estimator and threshold value used since they impact the effectiveness of denoising. Different estimators exist that are based on different threshold value quantization methods, viz., hard, soft, or semisoft thresholding.

Each estimator removes redundant coefficients using a nonlinear thresholding based on (4), where h is the noisy observation, ψ_m is the mother wavelet function, $m = (i, j)$ (2^i is the scale and j is the position of the wavelet basis), Ω is the thresholding estimator, q is the thresholding type, and T is the threshold used.

If x is an input signal, then the estimators used in this paper are defined based on (5)–(7), where μ is a parameter greater than 1, and the superscripts H, S, and SS denote hard, soft, and semisoft thresholding, respectively.

In nonlinear thresholding-based denoising methods [see (4)], translation invariance means that the basis $\{\psi_m = \psi_{i,j}\}_{i,j}$ is translation invariant $\forall m$, $\forall \tau \in \Phi$, where Φ is a lattice of $\Re^d$ and $d = 2$ for an image signal. While the Fourier basis is translation invariant, the orthogonal wavelet basis ψ_m is not (in either the continuous or discrete settings)

$$\hat{h} = \sum_{|\langle h,\psi_m\rangle|>T} \langle h, \psi_m\rangle \psi_m = \sum_m \Omega_T^q(\langle h, \psi_m\rangle)\psi_m \quad (4)$$

$$\Omega_T^H(x) = \begin{cases} x, & \text{if } |x| > T \\ 0, & \text{if } |x| \le T \end{cases} \quad (5)$$

$$\Omega_T^S(x) = \begin{cases} \operatorname{sgn}(x)\cdot(|x-T|), & \text{if } |x| > T \\ 0, & \text{if } |x| \le T \end{cases} \quad (6)$$

$$\Omega_T^{SS}(x) = \begin{cases} 0, & \text{if } |x| \le T \\ x, & \text{if } |x| > \mu T \\ \operatorname{sgn}(x)\cdot\frac{|x-T|}{\mu-1}, & \text{if } |x| > T, \text{otherwise.} \end{cases} \quad (7)$$

Image denoising using the traditional orthogonal wavelet transforms may result in visual artifacts. Some of these can be attributed to the lack of translation invariance of the wavelet basis. One method to suppress such artifacts is to “average out” the translation dependence, i.e., through “cycle spinning” as proposed by Coifman [27]

$$\Theta_{\mathrm{TI}}(h) = \frac{1}{|\Phi|}\cdot\sum_{\tau\in\Phi}\Theta(h_\tau)_{-\tau} \quad (8)$$

where $\forall \tau \in \Phi$, $\Theta_{\mathrm{TI}}(h) = \Theta_{\mathrm{TI}}(h_\tau)_{-\tau}$. This is called **cycle spinning** denoising. If we have an N-sample data, then pixel precision translation invariance is achieved by having N wavelet translation transforms (vectors) or $|\Phi| = N$.

Similar to cycle spinning denoising, thresholding-based translation invariant denoising can be defined as

$$\Theta_{\mathrm{TI}}(h) = \frac{1}{|\Phi|}\cdot\sum_{m,\tau\in\Phi}\Omega_T^q(\langle h, (\psi_m)_\tau\rangle)(\psi_m)_\tau. \quad (9)$$

The benefit of translation invariance over orthogonal thresholding is the SNR improvement afforded by the former. The problem with orthogonal thresholding is that it introduces oscillating artifacts that occur at random locations when τ changes. However, translation invariance significantly reduces these artifacts by the averaging process. A further improvement in SNR can be obtained by proper selection of the thresholding estimator.

IV. Face Image Restoration Methodology

The proposed restoration methodology is composed of an *online* and an *offline* process (see Fig. 4). The *online process* has two steps. First, each input face image is automatically classified into one of three degradation categories considered in this work: 1) class 1: fax compression, 2) class 2: fax compression, followed by printing and scanning, and 3) class 3: fax compression, followed by fax transmission and scanning. In actual implementation, the system will not know whether the input face image is degraded or not. If the input face image is the original (good quality) image, it is assigned a fourth category, i.e., 4) class 4: good quality. Based on this classification, a restoration algorithm with a predefined meta-parameter set associated with the nature of degradation of the input image, is invoked. Each meta-parameter set is deduced during the *offline process*.

A. Offline Process

Noniterative denoising methods (as those described above, viz., filtering and wavelet denoising with thresholding) derive a solution through an explicit numerical manipulation applied directly to the image in a single step. The advantages of noniterative methods are primarily ease of implementation and faster computation. Unfortunately, noise amplification is hard to control. Thus, when applied to degraded face images, they do not result in an acceptable solution. However, when they are applied iteratively and evaluated through a quality metric-based objective function, image reconstruction can be performed by optimizing this function. In our study, we employ such a scheme. At each step the system meta-parameters, i.e., 2-D FIR filter type/size, wavelet/thresholding type, and thresholding level, change incrementally within a predefined interval until the image quality of the reconstructed image is optimized in terms of some image distortion metric.

Mathematically, this can be expressed as follows. In each iteration i of the algorithm, let $\hat{h}$ be the noisy observation of a true 2-D image h_0, and $h_{\mathrm{l}}(p_{\mathrm{l}})$, $h_{\mathrm{nl}}(p_{\mathrm{nl}})$ be the estimated image after applying linear and nonlinear denoising, respectively,

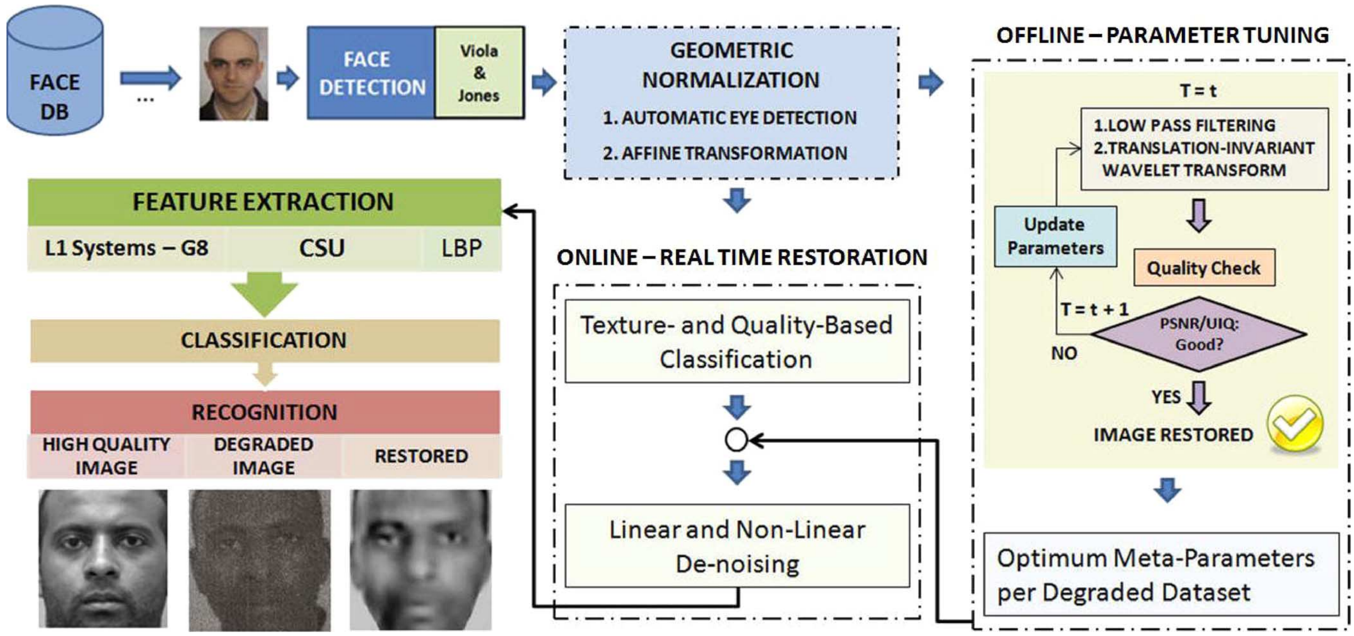

Fig. 4. Overview of the face image restoration methodology.

where $p_{\rm l} = \{f, \gamma\}$ denotes the set of linear denoising parameters, i.e., filter type and window size, and $p_{\rm nl} = \{w, q, T\}$ is the set of nonlinear parameters, i.e., wavelet type, thresholding type and level, respectively. Then, $\forall\ h \in \Xi$, where Ξ represents a dataset of N degraded images, given a finite domain $D = \{p_{\rm l}, p_{\rm nl}\}$ that represents the parameters employed (discrete or real numbers) and a quality metric function Q such that $Q : D \rightarrow R$, the proposed reconstruction method works by finding the parameter set $\overline{p}$ in D that maximizes Q

$$\overline{p} = \arg \max_{\{p_{\rm l}, p_{\rm nl}\} \in D} \{Q_i^{\rm l}[h_i^c, h_i^{\rm l}(p_{\rm l})],$$
$$\text{or } Q_i^{\rm nl}[h_i^c, h_i^{\rm nl}(p_{\rm nl})],$$
$$\text{or } Q_i^{\rm lnl}[h_i^c, h_i^{\rm nl}(h_i^{\rm l}(p_{\rm l}, p_{\rm nl}))]\}$$

where the terms involved correspond to filtering (noted as $\rm l$), nonlinear denoising (noted as $\rm nl$), and their combination (noted as $\rm lnl$).

This procedure is iterated until convergence (i.e., stability of the maximum quality) by altering the constrained parameters (window/wavelet/thresholding type) and updating the window size and threshold level in an incremental way. The maximum number of iterations is empirically set. For instance, a threshold value of more than 60 results in removing too much information content. The application of this process to a degraded training dataset results in an estimated parameter set for each image. The optimum meta-parameter set for each degraded training dataset is obtained by averaging. The derived meta-parameter sets are utilized in the online restoration process.

B. Online Process

In the online process (see Fig. 4), the degradation type of each input image is recognized by using a texture- and quality-based classification algorithm. First, the classifier utilizes the gray-tone spatial-dependence matrix, or cooccurrence matrix (COM) [28], which is the statistical relationship of a pixel's intensity to the intensity of its neighboring pixels. The COM measures the probability that a pixel of a particular gray level occurs at a specified direction and distance from its neighboring pixels. In this study, the main textural features extracted are inertia, correlation, energy, and homogeneity:

- **Inertia** is a measure of local variation in an image. A high inertia value indicates a high degree of local variation.
- **Correlation** measures the joint probability occurrence of the specified pixel pairs.
- **Energy** provides the sum of squared elements in the COM.
- **Homogeneity** measures the closeness of the distribution of elements in the COM to the COM diagonal.

These features are calculated from the cooccurrence matrix where pairs of pixels separated by a distance ranging from 1 to 40 in the horizontal direction are considered resulting in a total of 160 features per image (4 main textural features at 40 different offsets).

Apart from these textural features, image graininess is used as an additional image quality feature. Graininess is measured by the percentage change in image contrast of the original image before and after blurring is applied.[2] The identification of the degradation type of an input image is done by using the k-Nearest Neighbor (k-NN) method [29], [30] with $k = 5$. The online process restores the input image by employing the associated meta-parameter set (deduced in the offline process).

C. Computation Time

The *online restoration process* when using MATLAB on a Windows Vista 32-bit system with 4-GB RAM and Intel Core Duo CPU T9300 at 2.5 GHz, requires about 0.08 s for the k-NN classification and about 2.5 s for image denoising, i.e., a total time of less than 3 s per image.

[2]Available: http://www.clear.rice.edu/elec301/Projects02/artSpy/graininess.html

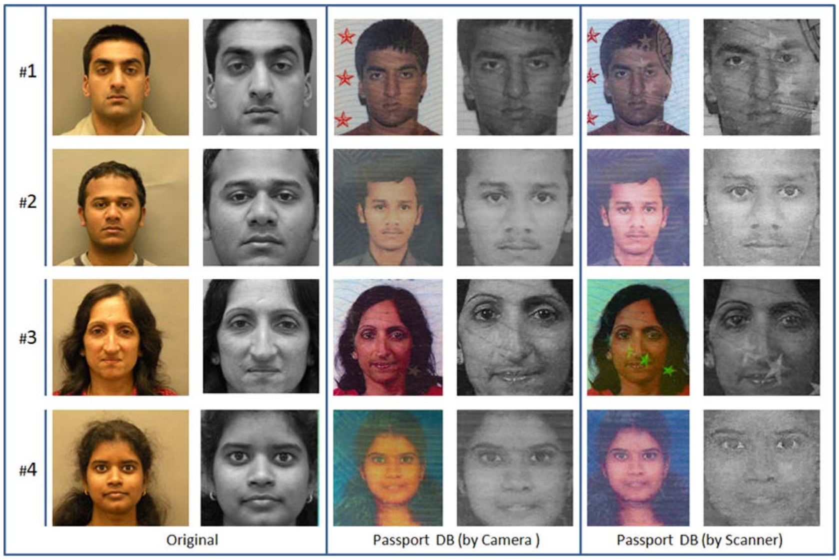

Fig. 5. Sample images of subjects in the three datasets of PassportDB.

V. Degraded Face Image Databases

In this section, we will describe the hardware used for 1) the acquisition of the high-quality face images, and 2) for printing, scanning, and faxing the face images (along with the associated software). We will also describe the live subject-capture setup used during the data collection process and the three degraded face image databases used in this paper.

1) Hardware and Subject-Capture Setup: A NIKON Coolpix P-80 digital camera was used for the acquisition of the high-quality face images (3648×2736) and an HP Office jet Pro L7780 system was used for printing and scanning images. The fax machine used was a Konica Minolta bizhub 501, in which the fax resolution was set to 600×600 dpi, the data compression method was MH/MR/MMR/JBIG, and transmission standard used for the fax communication line was super G3. The *Essential Fax* software was used to convert the scanned document of the initial nondegraded face photos into a PDF document with the fax resolution set to 203×196 dpi.

Our live subject-capture setup was based on the one suggested by the U.S. State Department, Bureau of Consular Affairs [31]. For the passport-capture setup we used the P-80 camera and the L7780 system. We acquired data from 28 subjects bearing passports from different countries, i.e., 4 from Europe, 14 from the United States, 5 from India, 2 from Middle East, and 3 from China; the age distribution of these participants was as follows: 20–25 (12 subjects), 25–35 (10 subjects), and over 35 (6 subjects). The database was collected over 2 sessions spanning approximately 10 days. In the beginning of the first session, the subjects were briefed about the data collection process after which they signed a consent document. During data collection, each subject was asked to sit $\sim$4 feet away from the camera. The data collection process resulted in the generation of three datasets, i.e., the NIKON Face Dataset (NFaceD) containing high-resolution face photographs from live subjects, the NIKON Passport Face Dataset (NPassFaceD) containing images of passport photos, and the HP Scanned Passport Face Dataset (HPassFaceD) containing face images scanned from the photo page of passports (see Fig. 5).

2) Experimental Protocol: Three databases were used in this paper (Fig. 6).

Passport Database: As stated above, the data collection process resulted in the generation of the *Passport Database (PassportDB)* composed of three datasets: 1) the NFaceD dataset that contains high-resolution face photographs from live subjects, 2) the NPassFaceD dataset that contains passport face images of the subjects acquired by using the P-80 camera, and 3) the HPassFaceD dataset that contains the passport face images of the subjects acquired by using the scanning mode of the L7780 machine.

In the case of NPassFaceD, three samples of the photo page of the passport were acquired for each subject. In the case of HPassFaceD, one scan (per subject) was sufficient to capture a reasonable quality mug-shot from the passport (Fig. 5).

Passport-Fax Database: This database was created from the *Passport Database* (Fig. 7). First, images in the Passport database were passed through four fax-related degradation scenarios. This resulted in the generation of four fax-passport datasets that demonstrate the different degradation stages of the faxing process when applied to the original passport photos: – **Dataset 1**: Each face image in the NPassFaceD/HPassFaceD datasets was placed in a Microsoft PowerPoint document. This document was then processed by the fax software producing a multipage PDF document with fax compressed face images. Each page of the document was then resized to +150%. Then, each face image was captured at a resolution of 600×600 dpi by using a screen capture utility software (SnagIt v8.2.3). – **Dataset 2**: Same as *Dataset 1*, but this time each page of the PowerPoint document was resized to +100%. Then each face image was captured at a resolution of 400×400 dpi. The purpose of employing this scenario was to study the effect of lower resolution of the passport face images on system performance. – **Dataset 3**: Following the same initial steps of *Dataset 1*, a multipage PDF document was produced with degraded images

DATABASES			
	DATASETS	DESCRIPTION	Number of [Subjects / Samples per Subject]
PASSPORT	NFaceD	Controlled Still Face Images	28 / 14
	NFacePassD	Passport Images (Nikon-Camera)	28 / 3
	HFacePassD	Passport Images (HP-Scanner)	28 / 1
FRGC2	EXP 1	Controlled Still Face Images	380 / 8
BOTH - FAXED	D1	• FAX Compression - Face Captured at 600x600 dpi	408 / 8
	D2	• FAX Compression - Face Captured at 400x400 dpi	
	D3	• FAX Compression • Print • Scan - Face Captured at 600x600 dpi	
	D4	• FAX Compression • SENT via FAX • Scan - Face Captured at 600x600 dpi	

Fig. 6. Description of the experimental protocol.

due to fax compression. The document was then printed and scanned at a resolution of 600×600 dpi. **– Dataset 4**: Again, we followed the same initial steps of *Dataset 1*. In this case, the PDF document produced was sent via an actual fax machine and each of the resulting faxed pages was then scanned at a resolution of 600×600 dpi.

FRGC2-Passport FAX Database: The primary goal of the *Face Recognition Grand Challenge* (FRGC) Database project was to evaluate the face recognition technology. In this work, we combined the FRGC dataset that has 380 subjects with our NFacePass dataset that consists of another 28 subjects. The extended dataset is composed of 408 subjects with eight samples per subject, i.e., 3264 high-quality facial images. The purpose was to create a larger dataset of high-quality face images that can be used to evaluate the restoration efficiency of our methodology in terms of identification performance, i.e., to investigate whether the restored face images can be matched with the correct identity in the augmented database. Following the process described for the previous database, four datasets were created and used in our experiments.

A. Face Image Matching Methodology

The salient stages of the proposed method are described below:

1) **Face Detection**: The Viola & Jones face detection algorithm [32] is used to localize the spatial extent of the face and determine its boundary.
2) **Channel Selection**: The images are acquired in the RGB color domain. Empirically, it was determined that in the majority of passports, the Green channel (RGB color space) and the Value channel (HSV color space) are less sensitive to the effects of watermarking and reflections from the lamination. These two channels are selected and then added, resulting in a new single-channel image. This step is beneficial when using the Passport data. With the fax data this step is not employed since the color images are converted to grayscale by the faxing process.
3) **Normalization**: In the next step, a geometric normalization scheme is applied to the original and degraded images after detection. The normalization scheme compensates for slight perturbations in the frontal pose. *Geometric normalization* is composed of two main steps: eye detection and affine transformation. Eye detection is based on a template matching algorithm. Initially, the algorithm creates a *global eye* from all subjects in the training set and then uses it for eye detection based on a cross correlation score between the global and the test image. Based on the eye coordinates obtained by eye detection, the canonical faces are constructed by applying an affine transformation as shown in Fig. 4. These faces are warped to a size of 300×300. The *photometric normalization* applied to the passport images before restoration is a combination of homomorphic filtering and histogram equalization. The same process is used for the fax compressed images before they are sent to the fax machine.
4) **Image Restoration**: The methodology discussed in Section IV is used. By employing this algorithm, we process the datasets described in Section V and create their reconstructed versions that are later used for quality evaluation and identity authentication. Fig. 8 illustrates the effect of applying the restoration algorithm on some of the Passport Datasets (1, 3, and 4), i.e., passport faces a) subjected to T.6 compression (FAX SW) and restored; b) subjected to T.6 compression, printed, scanned, and restored; and c) subjected to T.6 compression, sent via fax machine, then scanned and finally restored. Note that in Fig. 8, the degraded faces in the left column are the images obtained after face detection and before normalization.
5) **Face Recognition Systems**: Both commercial and academic software were employed to perform the face recognition experiments: 1) Commercial software *Identity*

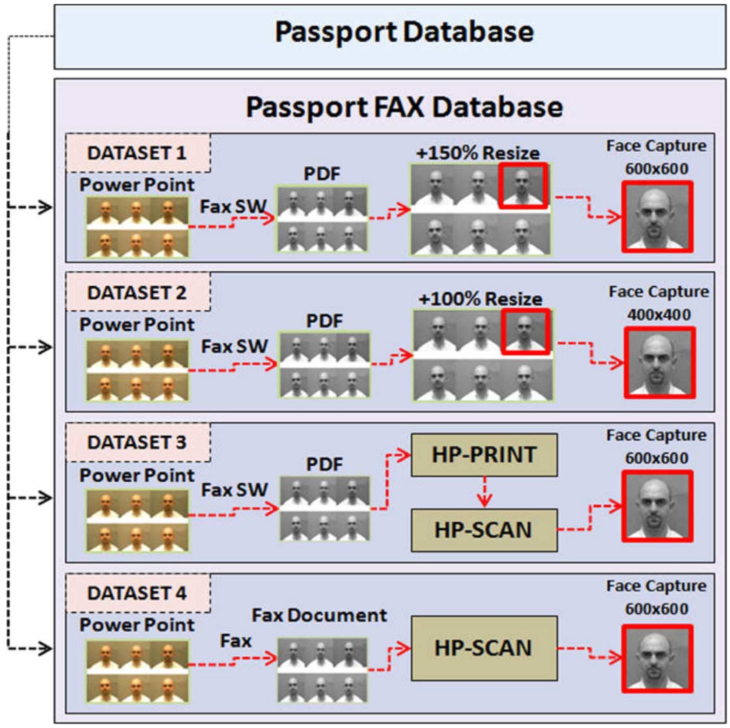

Fig. 7. Overview of the generation of the Passport FAX Database.

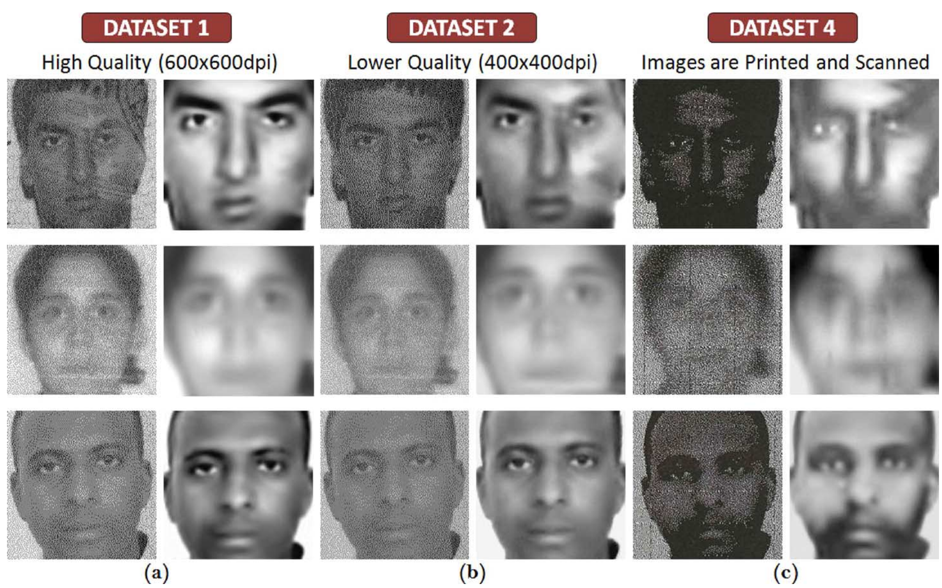

Fig. 8. Illustration of the effect of the proposed restoration algorithm. The input consists of (a) images subjected to fax compression and then captured at 600×600 dpi resolution; (b) images subjected to fax compression and then captured at 400×400 dpi resolution; (c) images subjected to fax compression then printed and scanned.

Tools G8 provided by L1 Systems;[3] 2) standard face recognition methods provided by the CSU Face Identification Evaluation System [8], including *Principle Components Analysis* (PCA) [33]–[35], *a combined Principle Components Analysis and Linear Discriminant Analysis algorithm* (PCA+LDA) [36], the *Bayesian Intrapersonal/Extra-personal Classifier* (BIC) using either the Maximum likelihood (ML) or the Maximum *a posteriori* (MAP) hypothesis [37] and the *Elastic Bunch Graph Matching* (EBGM) method [38]; and (3) *Local Binary Pattern* (LBP) method [39].

[3]Available: www.l1id.com

VI. Empirical Evaluation

The experimental scenarios investigated in this paper are the following: 1) evaluation of image restoration in terms of image quality metrics; 2) evaluation of the texture and quality based classification scheme; and 3) identification performance before and after image restoration.

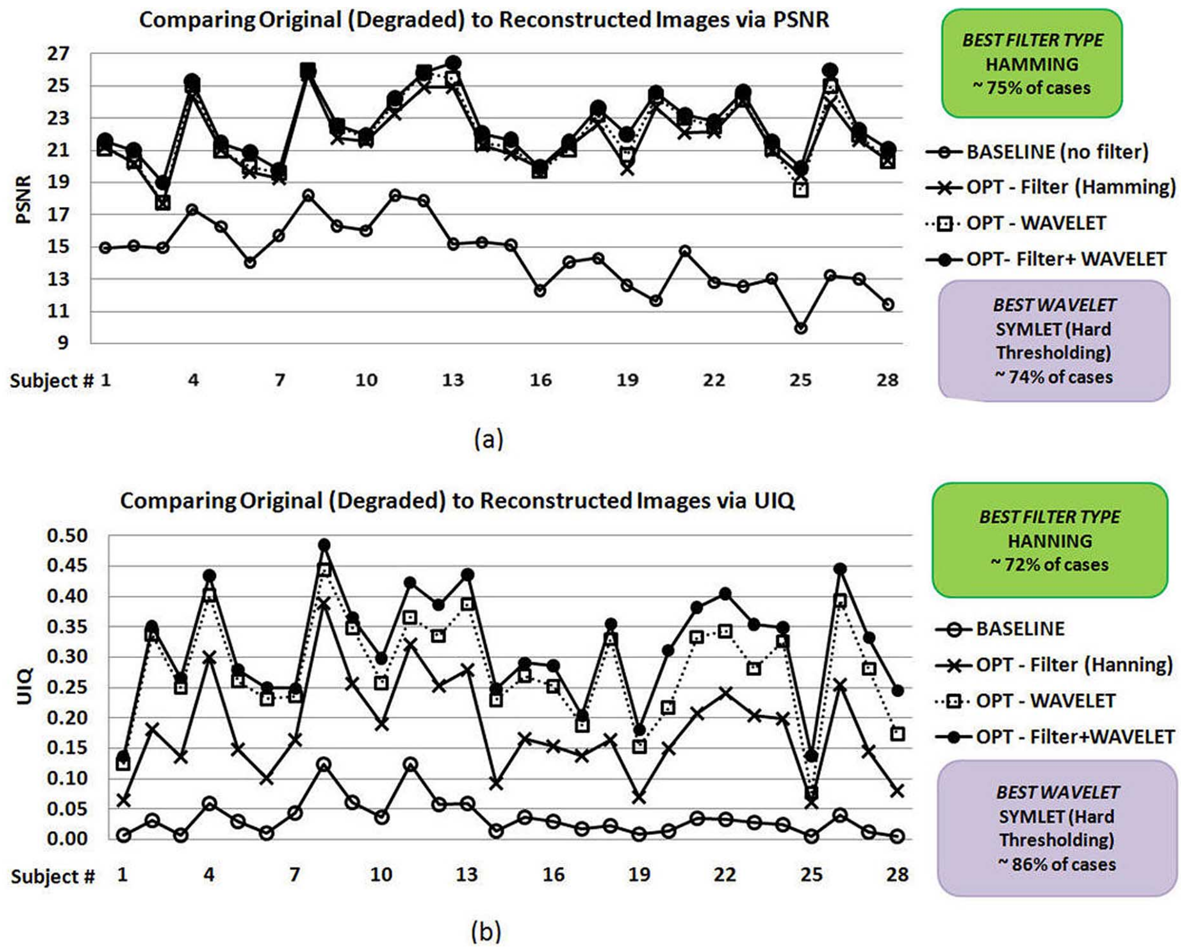

Fig. 9. Improvement in image quality as assessed by the PSNR and UIQ metrics. These metrics are computed by using the high-quality counterpart of each image as the "clean image."

A. Image Restoration Evaluation

In this experiment, we demonstrate that the combination of filtering and TI-denoising is essential for improving the quality of restoration. Due to the absence of the ground truth passport data (digital version of the face images before they are printed and placed on the passport), we compare the high-quality live face images of each subject against their degraded version (due to fax compression) in terms of the PSNR and UIQ metrics. We investigate whether 1) linear filtering (2-D finite impulse response (FIR) filters that used the windowing method), 2) denoising, or 3) their combination is a favorable choice for restoration.

In the *first experiment*, we tested seven windows, i.e., boxcar, Hamming, Hanning, Bartlett, Blackman, Kaiser, and Chebwin, and varied the window size from 3 to 60 in increments of 2. When PSNR is used, in the majority of the cases (~75%), the most efficient window for image restoration was Hamming. This is illustrated in Fig. 9(a). The same trend in results is observed when using the UIQ metric; however, in a majority of the cases (~72%), the most efficient window for image restoration was Hanning [Fig. 9(b)]. The main conclusion from this experiment is that image filtering does improve the quality of the degraded fax images.

In the *second experiment*, we determined the TI-wavelet parameter set that could offer the best tradeoff between image restoration (in terms of PSNR and UIQ) and computational complexity. Thus, in this experiment, we examined the use of different filters (Daubechies and Symlets), thresholding type (hard, soft, semisoft), and level of thresholding (from 5 to 75 in increments of 5). The *Daubechies* filters are minimal phase filters that generate wavelets which have a minimal support for a given number of vanishing moments. *Symlets* are also wavelets within a minimum size support for a given number of vanishing moments. However, they are as symmetrical as possible in contrast to the Daubechies filters which are highly asymmetrical. Experimental results show that in terms of the *average metric* (PSNR/UIQ) for all subjects, the best option is to employ Symlet wavelets with hard thresholding [see Fig. 9(a), (b)].

In the *third experiment*, we investigate the effect of combining filtering with denoising. Fig. 9(a) and (b) shows that, overall, the best option is to combine Hanning Filtering with Symlets (hard thresholding). We can see that in the baseline case, the quality of the degraded fax images before restoration is very low (almost zero in some cases). By using filtering, denoising, or both and employing the proposed iterative approach, the average image quality significantly improves. In the "best"

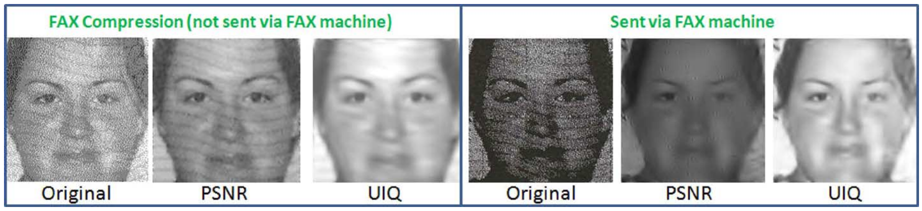

Fig. 10. Comparison of degraded images and their reconstructed counterparts after employing the proposed restoration method using PSNR/UIQ as quality metrics. UIQ appears to result in, at least visually, better images.

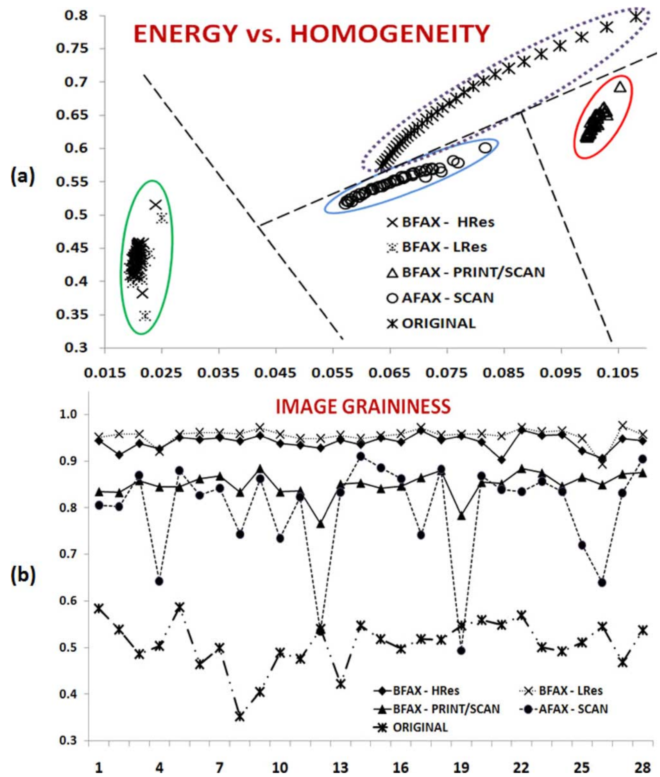

Fig. 11. (a) Clustering results when using textural features. (b) Importance of graininess in identifying the degraded datasets. B4FAX = Fax Compression (not sent via Fax machine). AFAX = sent via Fax machine.

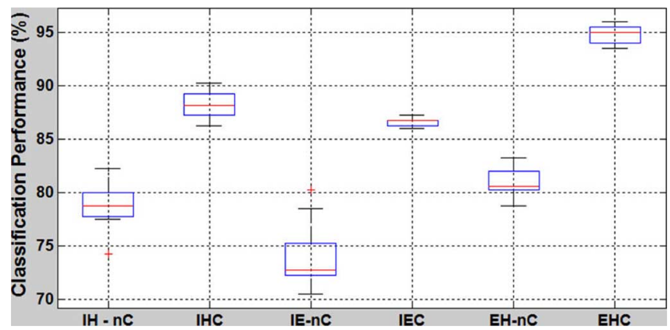

Fig. 12. Box plot of degradation classification performance results when using a combination of features. Note that the central mark (red line) is the median classification result over 10 runs, the edges of the box (blue) are the 25th and 75th percentiles, the whiskers (black lines) extend to the most extreme data points not considered outliers, and outliers (red crosses) are plotted individually. I = Inertia; H = Homogeneity; E = Energy; C = Contrast (Image Graininess); and nC = no usage of Contrast.

option, we achieve an average quality improvement of about 54% (PSNR), or approximately 7 times in terms of UIQ.

We note that the PSNR method does not provide as crisp a result as UIQ leading us to the following question: which metric should be trusted? We know that PSNR (as well as mean squared error) is one of the most widely used objective image quality/distortion metric, but is widely criticized as well, for not correlating well with perceived quality measurement. There are many other image quality measurements proposed in the literature, but most of them share a common error-sensitivity-based philosophy (motivated from psychological vision science research), i.e., human visual error sensitivities and masking effects vary in different spatial frequency, temporal frequency, and directional channels.

In our experiments, UIQ appears to be more robust in the selection of the best reconstructed image. Even though both PSNR and UIQ lead to the same conclusion (that the combination of image filtering and TI denoising is preferable), they converge to a different filtering window size and level of thresholding, and ultimately image restoration quality. Fig. 10 illustrates some cases where the reconstructed images based on PSNR were not as good as those that were based on UIQ. This is a general conclusion based on the results found across all degradation scenarios investigated in this paper.

Based on the results obtained in this set of experiments, we applied the iterative TI-wavelet restoration algorithm that combines Hanning filtering and Symlets with hard thresholding to both passport and passport-fax databases. The quality of the restoration was then tested by using the commercial face recognition software provided by L1 Systems.[4]

B. Evaluation of the Degradation Classification Algorithm

The *second* experimental scenario illustrates the efficiency of the degradation classification algorithm, i.e., the capability of identifying the degradation type of an input image. For each degraded dataset generated from the *FRGC2-Passport FAX Database* (Section V), a subset (approximately 22.5% of the training set that was used for the identification experiments) is used to extract the textural features as well as image graininess. Out of all the features considered here, the optimal ones in terms of performance are energy, homogeneity, and graininess. In Fig. 11(a), we see the clustering of these feature sets based on the nature of degradation of the input image. It is important to see that images in datasets 1 and 2 are within the same cluster. In contrast, datasets 3 and 4 form their own clusters. In addition, image graininess can be used to separate datasets (1,2) from (3,4).

[4]Available: http://www.l1id.com/

TABLE I
CLASSIFICATION RESULTS WHEN USING THE TEXTURAL- AND QUALITY-BASED CLASSIFICATION ALGORITHM. B4FAX = FAX COMPRESSION (NOT SENT VIA FAX MACHINE); LRes = LOW RESOLUTION; HRes = HIGH RESOLUTION; AFAX = SENT VIA FAX MACHINE; CL = CLASSIFICATION; EV = ERROR VARIANCE

FEATURES	DATASETS	CL (%)	EV
TEXTURAL	Class 1: [BFAX LRes/HRes]; Class 2: BFAX (Print and Scan); Class 3: AFAX	89.34	0.039
GRAININESS	Class 1: [BFAX LRes/HRes]; Class 2: BFAX (Print and Scan) and AFAX data	100.00	-
FUSED	Class 1: [BFAX LRes/HRes]; Class 2: BFAX (Print and Scan); Class 3: AFAX	96.84	0.038

TABLE II
PARTITIONING THE *FRGC2-PASSPORT* FAX DATABASE PRIOR TO APPLYING THE CSU FR ALGORITHMS

	TRAIN	TEST	GALLERY	PROBES
Subjects #	125	283	283	283
Images/Subject	4	4	0.25 (from TEST)	2-4 (from TEST)

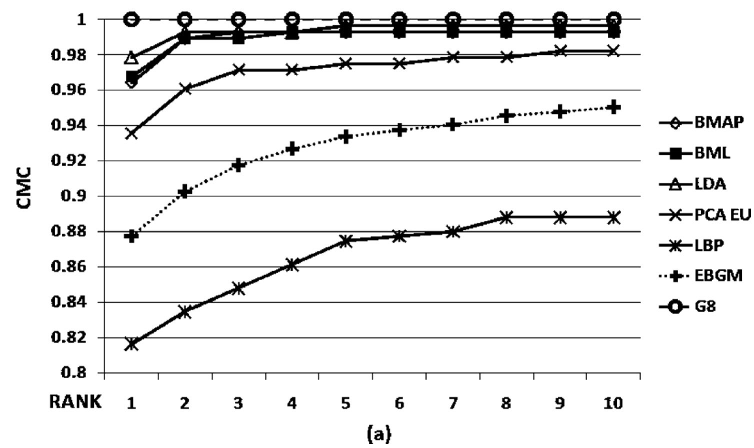

Fig. 13. Face identification results: High-quality versus high-quality face image comparison.

To test our classification algorithm, we used a dataset of $N = 108$ sample images (27 subjects $\times$ 4) for training and the four samples of the remaining (28th) subject for testing (1 subject $\times$ 4), where 4 in both cases represents one sample from each of the four classes involved. Thus, we performed a total of 28 experiments where the training and test datasets were resampled, i.e., in each experiment the data of a different subject (out of the 28) was used for testing. Each experiment was performed before and after fusing textural and image graininess features. The results are summarized in Table I. Note that if an image is misclassified, it will be subjected to the set of meta-parameters pertaining to the incorrect class.

We also applied our feature extraction algorithm on the original training set of the FRGC2 subset. Then, we randomly selected 100 samples from the original test set (see Table II) 10 times, and then applied feature extraction on each generated test subset. We performed the above process on the three degraded datasets that are generated from the original FRGC2 training/test sets, and performed 26 400 classification experiments in total. The outcome of these experiments is summarized Fig. 12 (box-plot results).

C. *Face Identification Experiments*

The *third* experimental scenario is a series of face identification tests which compare system performance resulting from the baseline (FRGC2-Passport FAX Database), degraded, and reconstructed face datasets. The goal here is to illustrate that the face matching performance improves with image restoration. For this purpose, we perform a two-stage investigation that involves 1) high-quality versus high-quality face image comparison (baseline), and 2) high-quality versus degraded face image comparison. In the *high-quality versus high-quality* tests, we seek to establish the baseline performance of each of the face recognition methods (academic and commercial) employed. In the *high-quality versus degraded* tests, we investigate the matching performance of degraded face images against their high-resolution counterparts.

Table II illustrates the way we split the *FRGC2-Passport FAX Database* to apply the CSU FR algorithms. For the G8 and LBP algorithms we used 4 samples of all the 408 subjects, and ran a 5-fold cross-validation where one sample per subject was used as the gallery image and the rest were used as probes. The *identification* performance of the system is evaluated through the cumulative match characteristic (CMC) curve. The CMC curve measures the $1 : m$ identification system performance, and judges the ranking capability of the identification system.

All the results before and after restoration are presented in Figs. 13–16. We can now evaluate the consistency of the results and the significant benefits of our restoration methodology in terms of face identification performance. For high-quality face images with no photometric normalization, the average *rank 1 score* of all the FR algorithms is ~93.43% (see Fig. 13). This average performance drops to 80.4% when fax compression images are used before restoration. After restoration, the average *rank 1 score* increases to 90.8% (12.94% performance improvement). When the fax compressed images are also printed,

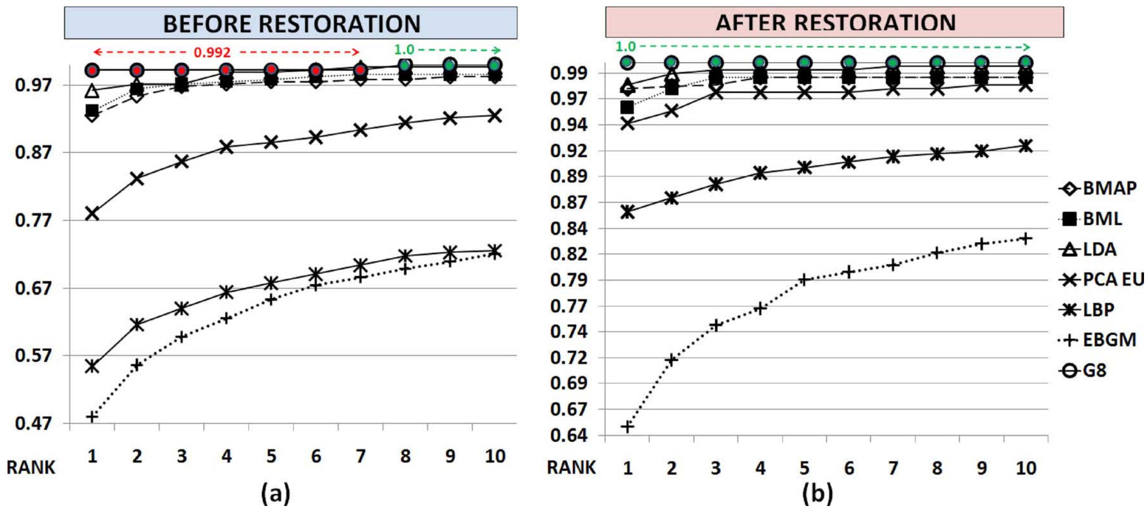

Fig. 14. Face identification results: High-quality versus Fax compressed images.

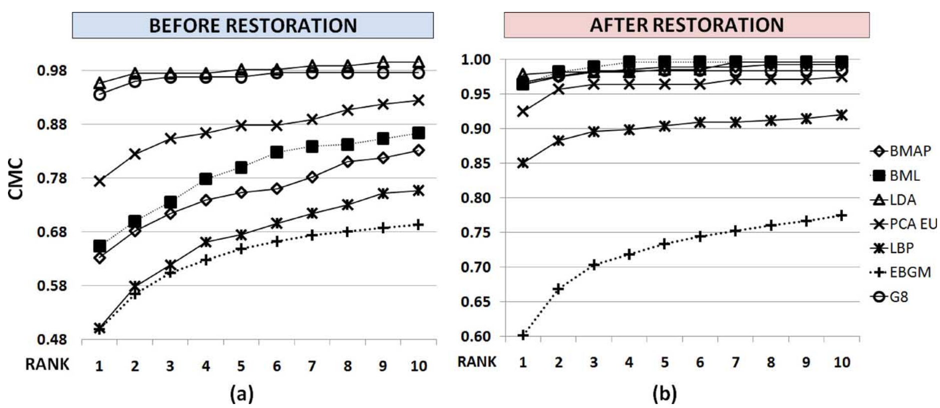

Fig. 15. Face identification results: High-quality versus Fax compressed images which have been printed and scanned.

the performance drops further to 70.8% before restoration, but increases to 89.3% after restoration (26.13% performance improvement). Finally, when the most degraded images were used (images sent via a fax machine) the average *rank 1 score* across all the algorithms drops to 58.7% before restoration while after restoration it goes up to 81.2%. It is interesting to note that the identification performance of the high-quality images is comparable to that of the restored degraded images. Note that each face identification algorithm performs differently, and in some cases (e.g., G8), the performance is optimal for both raw and restored images (in the case of fax compression) achieving a 100% identification rate at rank 1. The consistency in improving recognition performance indicates the significance of the proposed face image restoration methodology.

VII. Conclusions and Future Work

We have studied the problem of image restoration of severely degraded face images. The proposed image restoration algorithm compensates for some of the common degradations encountered in a law-enforcement scenario. The proposed restoration method consists of an offline mode (image restoration is applied iteratively, resulting in the optimum meta-parameter sets), where the objective function is based on two different image quality metrics. The online restoration mode uses a classification algorithm to determine the nature of the degradation in the input image, and then uses the meta-parameter set identified in the offline mode to restore the degraded image. Experimental results show that the restored face images not only have higher image quality, but they also lead to higher recognition performance than their original degraded counterparts.

Commercial face recognition software may have their own internal normalization schemes (geometric and photometric) that cannot be controlled by the end-user, and this can result in inferior performance when compared to some academic algorithms (i.e., LDA) when restoration is employed. For example, when G8 was used on fax compressed data, the identification performance was 79.2% while LDA resulted in a 91.4% matching accuracy. In both cases, the restoration helped, yet LDA (97.9%) performed better than G8 (93.6%). Since the preprocessing stage of the noncommercial algorithms can be better controlled than commercial ones, several academic algorithms were found to be comparable in performance to the commercial one after restoration.

The proposed image restoration approach can potentially discard important textural information from the face image. One possible improvement could be the use of super-resolution algorithms that learn *a prior* on the spatial distribution of the image

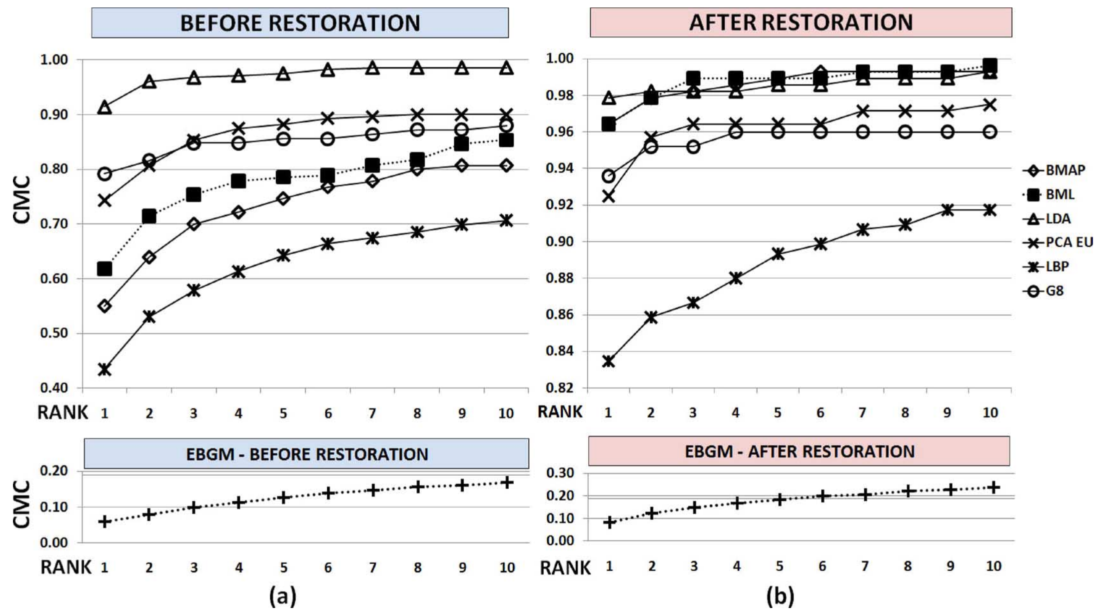

Fig. 16. Face identification results: High-quality versus images that are sent via a Fax machine and then scanned. Note that the EBGM method is illustrated separately because it results in very poor matching performance. This could be implementation-specific and may be due to errors in detecting landmark points.

gradient for frontal images of faces [19]. Another future direction is to extend the proposed approach to real surveillance scenarios in order to restore low quality images. Finally, another area that merits further investigation is the better classification of degraded images. Such an effort will improve the integrity of the overall restoration approach.

ACKNOWLEDGMENT

The authors would like to thank researchers at Colorado State University for their excellent support in using the Face Evaluation Toolkit. They are grateful to Z. Jafri, C. Whitelam, and A. Jagannathan at West Virginia University for their valuable assistance with the experiments.

REFERENCES

[1] T. Bourlai, A. Ross, and A. Jain, "On matching digital face images against scanned passport photos," in *Proc. First IEEE Int. Conf. Biometrics, Identity and Security (BIDS)*, Tampa, FL, Sep. 2009.

[2] P. J. Phillips, W. T. Scruggs, A. J. O'Toole, P. J. Flynn, K. W. Bowyer, C. L. Schott, and M. Sharpe, "FRVT 2006 and ICE 2006 large-scale experimental results," *IEEE Trans. Pattern Anal. Mach. Intell.*, vol. 32, no. 5, pp. 831–846, May 2010.

[3] S. K. Zhou, R. Chellappa, and W. Zhao, *Unconstrained Face Recognition*. New York: Springer, 2006.

[4] R. Floyd and L. Steinberg, "An adaptive algorithm for spatial grey scale," in *Proc. Society of Information Display*, 1976, vol. 17, pp. 75–77.

[5] Z. Wang and A. C. Bovik, "A universal image quality index," *IEEE Signal Process. Lett.*, vol. 9, no. 3, pp. 81–84, Mar. 2002.

[6] P. J. Phillips, P. J. Flynn, T. Scruggs, K. W. Bowyer, J. Chang, K. Hoffman, J. Marques, J. Min, and W. Worek, "Overview of the face recognition grand challenge," in *Proc. Computer Vision and Pattern Recognition Conf.*, Jun. 2005, vol. 1, pp. 947–954.

[7] T. Ahonen, A. Hadid, and M. Pietikinen, "Face recognition with local binary patterns: Application to face recognition," in *Proc. Eur. Conf. Computer Vision (ECCV)*, Jun. 2004, vol. 8, pp. 469–481.

[8] D. S. Bolme, J. R. Beveridge, M. L. Teixeira, and B. A. Draper, "The CSU face identification evaluation system: Its purpose, features and structure," in *Proc. Int. Conf. Computer Vision Systems*, Apr. 2003, pp. 304–311.

[9] H. C. Andrews and B. R. Hunt, *Digital Image Restoration*. Englewood Cliffs, NJ: Prentice-Hall, 1977.

[10] M. R. Banham and A. K. Katsaggelos, "Digital image restoration," *IEEE Signal Process. Mag.*, vol. 14, no. 2, pp. 24–41, Aug. 2002 [Online]. Available: http://dx.doi.org/10.1109/79.581363

[11] J. G. Nagy and D. P. O'Leary, "Restoring images degraded by spatially-variant blur," *SIAM J. Sci. Comput.*, vol. 19, pp. 1063–1082, 1996.

[12] M. Figueiredo and R. Nowak, "An EM algorithm for wavelet-based image restoration," *IEEE Trans. Image Process.*, vol. 12, no. 8, pp. 906–916, Aug. 2003.

[13] J. Bioucas Dias and M. Figueiredo, "A new TwIST: Two-step iterative shrinkage/thresholding algorithms for image restoration," *IEEE Trans. Image Process.*, vol. 16, no. 12, pp. 2992–3004, Dec. 2007.

[14] A. M. Thompson, J. C. Brown, J. W. Kay, and D. M. Titterington, "A study of methods of choosing the smoothing parameter in image restoration by regularization," *IEEE Trans. Pattern Anal. Mach. Intell.*, vol. 13, no. 4, pp. 326–339, Apr. 1991.

[15] M. I. Sezan and A. M. Tekalp, "Survey of recent developments in digital image restoration," *Opt. Eng.*, vol. 29, no. 5, pp. 393–404, 1990 [Online]. Available: http://link.aip.org/link/?JOE/29/393/1

[16] P. H. Hennings-Yeomans, S. Baker, and B. V. Kumar, "Simultaneous super-resolution and feature extraction for recognition of low-resolution faces," in *Proc. Computer Vision and Pattern Recognition (CVPR)*, Jun. 2008, pp. 1–8.

[17] P. H. Hennings-Yeomans, B. V. K. V. Kumar, and S. Baker, "Robust low-resolution face identification and verification using high-resolution features," in *Proc. Int. Conf. Image Processing (ICIP)*, Nov. 2009, pp. 33–36.

[18] W. T. Freeman, T. R. Jones, and E. C. Pasztor, "Example based super-resolution," *IEEE Comput. Graph. Applicat.*, vol. 22, no. 2, pp. 56–65, Mar./Apr. 2002.

[19] S. Baker and T. Kanade, "Hallucinating faces," in *Proc. Fourth Int. Conf. Auth. Face and Gesture Rec.*, Grenoble, France, 2000.

[20] M. Elad and A. Feuer, "Super-resolution reconstruction of image sequences," *IEEE Trans. Pattern Anal. Mach. Intell.*, vol. 21, no. 9, pp. 817–834, Sep. 1999.

[21] N. Ramanathan and R. Chellappa, "Face verification across age progression," *IEEE Trans. Image Process.*, vol. 15, no. 11, pp. 3349–3362, Nov. 2006.

[22] V. V. Starovoitov, D. Samal, and B. Sankur, "Matching of faces in camera images and document photographs," in *Proc. Int. Conf. Acoustic, Speech, and Signal Processing*, Jun. 2000, vol. IV, pp. 2349–2352.

[23] V. V. Starovoitov, D. I. Samal, and D. V. Briliuk, "Three approaches for face recognition," in *Proc. Int. Conf. Pattern Recognition and Image Analysis*, Oct. 2002, pp. 707–711.

[24] S. K. Mohideen, S. A. Perumal, and M. M. Sathik, "Image de-noising using discrete wavelet transform," *Int. J. Comput. Sci. Netw. Security*, vol. 8, no. 1, pp. 213–216, Jan. 2008.

[25] Q. Huynh-Thu and M. Ghanbari, "Scope of validity of PSNR in image/video quality assessment," *Electron. Lett.*, vol. 44, no. 13, pp. 800–801, 2008.

[26] D. Donoho and I. Johnstone, "Ideal spatial adaptation via wavelet shrinkage," *Biometrika*, vol. 81, pp. 425–455, 1994.

[27] R. R. Coifman and D. L. Donoho, "Translation-invariant de-noising," in *Wavelets and Statistics*. New York: Springer-Verlag, 1994, vol. 103, Springer Lecture Notes, pp. 125–150.

[28] R. M. Haralick, K. Shanmugam, and I. Dinstein, "Textural features for image classification," *IEEE Trans. Syst., Man, Cybern.*, vol. SMC-3, no. 6, pp. 610–621, Nov. 1973.

[29] T. M. Cover and P. E. Hart, "Nearest neighbor pattern classification," *IEEE Trans. Inform. Theory*, vol. 13, no. 1, pp. 21–27, Jan. 1967.

[30] E. Fix and J. L. Hodges, Discriminatory Analysis, Nonparametric Discrimination: Consistency Properties USAF School of Aviation Medicine, Randolph Field, TX, Tech. Rep. 4, 1951.

[31] Setup and Production Guidelines for Passport and Visa Photographs U.S. Department of State, 2009 [Online]. Available: http://travel.state.gov/passport/get/get_873.html

[32] P. A. Viola and M. J. Jones, "Robust real-time face detection," *Int. J. Comput. Vis.*, vol. 57, no. 2, pp. 137–154, 2004.

[33] L. Sirovich and M. Kirby, "Application of the Karhunen-Loeve procedure for the characterization of human faces," *IEEE Trans. Pattern Anal. Mach. Intell.*, vol. 12, no. 1, pp. 103–108, Jan. 1990.

[34] M. Turk and A. Pentland, "Eigenfaces for recognition," *J. Cognitive Neurosci.*, vol. 3, no. 1, pp. 71–86, 1991.

[35] A. P. Devijver and J. Kittler, *Pattern Recognition: A Statistical Approach*. Englewood Cliffs, NJ: Prentice-Hall, 1982.

[36] P. Belhumeur, J. Hespanha, and D. J. Kriegman, "Eigenfaces vs. fisherfaces: Recognition using class specific linear projection," *IEEE Trans. Pattern Anal. Mach. Intell.*, vol. 19, no. 7, pp. 711–720, Jul. 1997.

[37] M. Teixeira, "The Bayesian Intrapersonal/Extrapersonal Classifier," Master's thesis, Colorado State University, Fort Collins, CO, 2003.

[38] L. Wiskott, J.-M. Fellous, N. Kruger, and C. V. D. Malsburg, "Face recognition by elastic bunch graph matching," *IEEE Trans. Pattern Anal. Mach. Intell.*, vol. 19, no. 7, pp. 775–779, Jul. 1997.

[39] M. Pietikinen, "Image analysis with local binary patterns," in *Proc. Scandinavian Conf. Image Analysis*, Jun. 2005, pp. 115–118.

Thirimachos Bourlai (M'10) received the Diploma (M.Eng. equivalent) in electrical and computer engineering from the Aristotle University of Thessaloniki, Greece, in 1999, the M.Sc. degree in medical imaging (with distinction) from the University of Surrey, U.K., in 2002 under the supervision of Prof. M. Petrou. He received the Ph.D. degree (full scholarship) in the field of face recognition and smart cards, in 2006, in a collaboration with OmniPerception Ltd. (U.K.), and his Postdocorate in multimodal biometrics, in August 2007, both under the supervision of Prof. J. Kittler.

He worked as a Postdoctoral researcher in a joint project between the University of Houston and the Methodist Hospital (Department of Surgery) at Houston, TX, in the fields of thermal imaging and computational physiology. From February 2008 to December 2009 he worked as a Visiting Research Assistant Professor at West Virginia University (WVU), Morgantown. Since January 2010 he has been a Research Assistant Professor at WVU. He is supervising the eye detection team, has been involved in various projects in the fields of biometrics, and multispectral imaging, and authored several book chapters, journals and conference papers. His areas of expertise are image processing, pattern recognition, and biometrics.

Arun Ross (S'00–M'03–SM'10) received the B.E. (Hons.) degree in computer science from BITS, Pilani, India, in 1996, and the M.S. and Ph.D. degrees in computer science and engineering from Michigan State University, in 1999 and 2003, respectively.

Between 1996 and 1997, he was with Tata Elxsi (India) Ltd., Bangalore. He also spent three summers (2000–2002) at Siemens Corporate Research, Inc., Princeton working on fingerprint recognition algorithms. He is currently an Associate Professor in the Lane Department of Computer Science and Electrical Engineering at West Virginia University. His research interests include pattern recognition, classifier fusion, machine learning, computer vision, and biometrics. He is the coauthor of *Handbook of Multibiometrics* and coeditor of *Handbook of Biometrics*. He is an Associate Editor of the IEEE TRANSACTIONS ON IMAGE PROCESSING and the IEEE TRANSACTIONS ON INFORMATION FORENSICS AND SECURITY.

Dr. Ross is a recipient of NSF's CAREER Award and was designated a Kavli Frontier Fellow by the National Academy of Sciences in 2006.

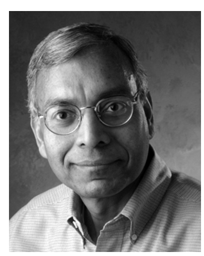

Anil K. Jain (S'70–M'72–SM'86–F'91) is a university distinguished professor in the Department of Computer Science and Engineering at Michigan State University. His research interests include pattern recognition and biometric authentication. The holder of six patents in the area of fingerprints, he is the author of a number of books, including *Handbook of Fingerprint Recognition* (2009), *Handbook of Biometrics* (2007), *Handbook of Multibiometrics* (2006), *Handbook of Face Recognition* (2005), *BIOMETRICS: Personal Identification in Networked Society* (1999), and *Algorithms for Clustering Data* (1988).

Dr. Jain received the 1996 IEEE TRANSACTIONS ON NEURAL NETWORKS Outstanding Paper Award and the Pattern Recognition Society best paper awards in 1987, 1991, and 2005. He served as the editor-in-chief of the IEEE TRANSACTIONS ON PATTERN ANALYSIS AND MACHINE INTELLIGENCE (1991–1994). He is a fellow of the AAAS, ACM, IEEE, IAPR, and SPIE. He has received Fulbright, Guggenheim, Alexander von Humboldt, IEEE Computer Society Technical Achievement, IEEE Wallace McDowell, ICDM Research Contributions, and IAPR King-Sun Fu awards. ISI has designated him a highly cited researcher. According to Citeseer, his book *Algorithms for Clustering Data* (Prentice-Hall, 1988) is ranked #93 in most cited articles in computer science. He served as a member of the Defense Science Board and The National Academies committees on Whither Biometrics and Improvised Explosive Devices.